Neuroscience 130 (2005) 239–247

FREQUENCY BANDS AND SPATIOTEMPORAL DYNAMICS OF β BURST STIMULATION INDUCED AFTERDISCHARGES IN HIPPOCAMPUS *IN VIVO*

J. E. MIKKONEN AND M. PENTTONEN*

A. I. Virtanen Institute for Molecular Sciences, University of Kuopio, P.O. Box 1627, FIN-70211 Kuopio, Finland

Abstract—Temporal and spatial characteristics of hippocampal neuronal network activation are modified during epileptiform afterdischarges. We developed a β burst stimulation protocol to investigate subregional variations and substrates of rhythmic population spike discharges *in vivo* in urethane anesthetized Wistar rat hippocampus with a 14-electrode recording array and extracellular single electrode recordings. Our 64 pulse β burst stimulation protocol was constructed from electrical pulses delivered at intervals corresponding to β (14–25 Hz), Δ (2 Hz), and slow (0.5 Hz) frequencies. In each experiment these interleaved pulses were all repeated four times with unchanged intervals. Stimulation of either perforant path or fimbria fornix induced a prolonged afterdischarge pattern peaking at 200 Hz fast, 20 Hz β, and 2 Hz Δ frequencies. Analysis of variance confirmed that the response pattern of the discharges remained constant regardless of the stimulation β frequency. Within the afterdischarge the fast frequencies were restricted to independent hippocampal subfields whereas β and slow frequencies correlated across the subfields. Current source density (CSD) analysis revealed that the original signal propagation through subfields of the hippocampus was compromised during the β burst stimulation induced afterdischarge. In addition, the CSD profile of the epileptiform afterdischarge was consistently similar across the different experiments. Time-frequency analysis revealed that the β frequency afterdischarge was initiated and terminated at higher γ (30–80 Hz) frequencies. However, the alterations in the CSD profile of the hippocampus coincided with the β frequency dominated discharges. We propose that hippocampal epileptiform activity at fast, β and Δ frequencies represents coupled oscillators at respectively increasing spatial scales in the hippocampal neuronal network *in vivo*.

Key words: extracellular, neuronal network, synchrony, coupled oscillator.

Investigation of the transition between normal and abnormal brain states provides insight into the network architecture and function of the brain. One way to understand neuronal networks is to examine disturbances in the electrical network of the brain during epilepsy or epileptiform brain states. Thus, periodic ultrasynchronous discharges of large neuronal ensembles are the hallmark of various epileptic conditions (McCormick and Contreras, 2001), and the study of the initial conditions of such discharges can provide information on normal brain function, as well as elucidate the mechanisms involved in the generation of epileptiform activity. Hippocampus is an important focus of epileptic activity in humans and in some animal models of temporal lobe epilepsy (McCormick and Contreras, 2001; Jefferys, 2003). Therefore, it seemed appropriate to study the mechanisms of the emergence of afterdischarges in the hippocampal neuronal networks. Epilepsy related functional reorganization of the hippocampal network can be examined via the electrical properties of the network. To date, the *in vivo* methodology of local field potential recording offers the most complete tool to investigate normal or pathological fast network interactions in the intact brain.

Within normal brain states, the β and Δ frequencies have been associated with epilepsy prone internal brain activity, such as 14 Hz sleep spindles in the thalamus (Steriade et al., 1993), synchronized activity in prefrontal cortex (Liang et al., 2002), and hippocampal memory consolidation during slow wave sleep (Buzsaki, 1989; Sirota et al., 2003). Bragin et al. (1997a), Amzica and Steriade (1999), and Hirai et al. (1999) have also reported β frequencies occurring in epileptic conditions *in vivo*. It has been claimed that β frequency stimulation can either induce epileptiform activity (Somjen et al., 1985; Lothman and Williamson, 1992) or that after the epileptiform synchrony has developed, one of its hallmarks is β frequency bursting (Pare et al., 1992; Bragin et al., 1997a; Amzica and Steriade, 1999; Hirai et al., 1999; Medvedev et al., 2000). However, only a few experiments have been conducted linking the β frequency induction of paroxysmal afterdischarges into the epileptiform β frequency outcome of the stimulation (Amzica and Steriade, 1999). Furthermore, Bikson et al. (2003) have demonstrated that paroxysmal β frequencies are at least initially accompanied with fast, >80 Hz, oscillations whereas Pare et al. (1992) and Steriade and Contreras (1998) have reported Δ frequencies co-occurring with β frequencies in already epileptiform conditions.

A systematic investigation of an epileptiform afterdischarge with time-sensitive interactions involving more than two frequency bands would provide novel information about the temporal structure and frequency division of the afterdischarge and facilitate the understanding of the mechanisms behind the development of the epileptiform afterdischarge. Here we report brief β burst stimulation induced epileptiform afterdischarges in rat hippocampus *in vivo* co-occurring at anatomically distinct scales and at three frequency bands.

*Corresponding author. Tel: +358-17-162345; fax: +358-17-163030.
E-mail address: markku.penttonen@uku.fi (M. Penttonen).
Abbreviations: CA1, cornu ammonis region 1; CA3, cornu ammonis region 3; CSD, current source density; DG, dentate gyrus; SR, stratum radiatum.

0306-4522/05$30.00+0.00
doi:10.1016/j.neuroscience.2004.08.039

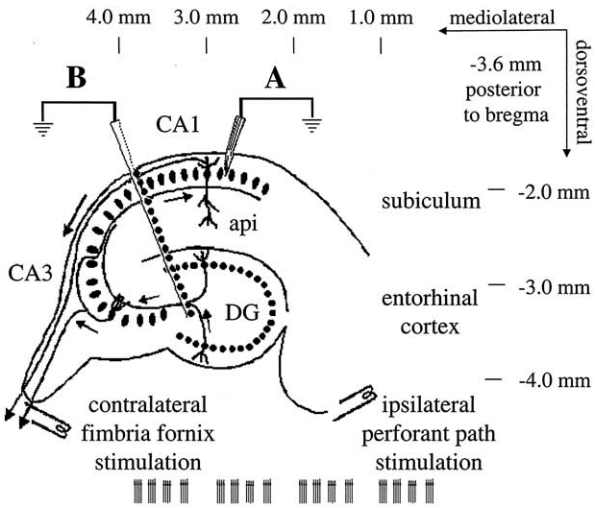

Fig. 1. Structure of the hippocampus including an illustration of the recording and stimulation sites within the hippocampus. Recordings were performed with a single electrode from CA1 2.2 mm mediolaterally from the midline (A) or with a 16 channel silicon probe in a 30° angle 4 mm mediolaterally from the midline (B). CA1 pyramidal cell layer (CA1), CA1 apical dendrites (api), and the granule cell layer of DG are shown in the hippocampus. Stimulation electrodes were inserted into contralateral fimbria fornix (A and B) and into ipsilateral perforant path (B) for *in vivo*-periodic electrical β burst stimulation at twice the threshold necessary to evoke a population spike. The temporal structure of the stimulation (14–25 Hz, 2 Hz, and 0.5 Hz) is schematically illustrated at the bottom of the figure.

EXPERIMENTAL PROCEDURES

Animals

Experiments were conducted on 20 male Kuopio Wistar rats (250–350 g) anesthetized with 1.1–1.4 g/kg urethane. The experiments were designed in order to minimize the number of animals used and their suffering. The methods used in the experiments follow the international guidelines on the ethical use of experimental animals and were approved by the Provincial Government of Eastern Finland (approval number 99–61).

Surgical preparation

Animals were placed in a stereotaxic instrument, the scalp was removed, and small bone windows were drilled above the target structures. Two separate paradigms were used in the recordings, illustrated as A and B in Fig. 1. Paradigm A consisted of single electrode (60 μm tungsten wire) recordings of local field potentials from the pyramidal cell layer of the CA1 field of the hippocampus (−3.6 mm anteroposterior and −2.2 mm lateral to bregma, 15 animals). Paradigm B consisted of 14 channel (16-channel silicon probe with 100 μm recording site separation, courtesy of Center for Neural Communication Technology, University of Michigan Electrical Engineering and Computer Science Department, Ann Arbor, MI, USA) recordings perpendicular to the hippocampal subfields (−3.6 mm anteroposterior and −4.0 mm lateral to bregma with a 30° angle toward midline (five animals) to monitor principal cell layers of dentate gyrus (DG) and CA1 as well as CA1 apical dendrites. Due to the limitations of a vertical recording array we were restrained to record DG and CA1 omitting the CA3 region connecting the recorded areas. In both paradigms, a pair of stainless steel wires (100 μm in diameter) with 0.2–0.4 mm tip separation was placed in the fimbria fornix (−1.3 mm anteroposterior and +1.0 mm lateral to bregma, and −4.0 mm ventral from cortical brain surface) to stimulate antidromically the commissural efferents of the contralateral CA3 region. In paradigm B, an additional pair of steel wires was placed −7.0 mm anteroposterior and −4.0 mm lateral to bregma and −3.0 mm ventral from cortical brain surface to stimulate the perforant path.

Recording and stimulations

We used 0.2 ms electrical pulse stimulation (Master8 pulse generator and Iso-flex stimulus isolator; A.M.P.I, Jerusalem, Israel) at an intensity that was twice the threshold capable of inducing population spikes in more than two consecutive trials for both stimulation sites. The stimulation intensity was 300–600 μA. Vertical positioning to the CA1 pyramidal layer for the single channel extracellular and 14-channel silicon probe recordings was estimated from the polarity of the field response, the shape and firing patterns of the population spikes (Markram et al., 1997), and from the latency of the evoked field response and population spikes. Typically the CA1 pyramidal layer was located −2.0±0.1 mm below the cortical surface. Additionally, we used current source density (CSD) analysis to confirm the positions of the hippocampal subfields in the silicon probe experiments. Two stainless steel watch screws, driven into the bone above the cerebellum served as indifferent and ground electrodes in the recordings.

We used a modified stimulation paradigm from Mikkonen et al. (2002) with different frequency ranges. Briefly, the stimulation consisted of four 0.2 ms pulses delivered at frequencies from 14 to 25 Hz with two underlying frequencies at 2 Hz and 0.5 Hz. Thus, we constructed a hierarchical stimulation that consisted of three interwoven frequency bands, slow, Δ, and β, each repeating four times and yielding a total stimulation of 64 pulses (Fig. 1). In order to maintain the stimulation intensity at a comparable level across the stimulations the β stimulation frequency was designed to cover merely central part of the frequency band (14–25 Hz out of 10–30 Hz). The stimulation was repeated every 10 min. Every two hours there was an additional 30 min recovery period with no stimulation. If afterdischarges had not developed after two hours of stimulations, the number of stimulation pulses at each β sequence was increased to six. The stimulation paradigm was designed using frequency ranges co-occurring in slow wave sleep (Buzsaki, 1989) and epilepsy (Timofeev et al., 1998; Amzica and Steriade, 1999). Furthermore, grouping stimulation pulses interleaved with silent episodes provided a timeframe for the examination of the early development of paroxysmal afterdischarges (Mikkonen et al., 2002).

The multichannel extracellular signals were first 500-fold amplified using Multichannel Systems (Reutlingen, Germany) amplifiers (two MPA-8s and one PA-32-D). The signals were then filtered between 0.1 and 5000 Hz (PA-32-D). Single electrode recordings were filtered between 0.1 and 6000 Hz using Cyberamp380 (Axon Instruments, Union City, CA, USA). Finally, all the signals were sampled with 16-bit precision (Digidata 1320A; Axon Instruments) at 10 kHz (single channel recordings) or 12.5 kHz (multichannel recordings). The data were stored on a computer hard disk using Axoscope 8.0 data acquisition software (Axon Instruments). The data analyses were performed offline using Clampfit 9.0 (Axon Instruments), Matlab 6.5 (MathWorks Inc., Natick, MA, USA), and SPSS 11 for Windows (SPSS Inc., Chicago, IL, USA).

The single channel extracellular signal recorded from CA1 pyramidal layer was used to compare instantaneous firing frequencies within afterdischarges against stimulation frequencies (Mikkonen et al., 2002). The signal was digitally low-pass filtered (finite impulse response filter) at 500 Hz, downsampled to 1 kHz, and subjected to an additional high-pass finite impulse response filtering at 100 Hz to distinguish population spikes.

Data analyses

The instantaneous frequency was calculated from the interval between the negative peaks of two consecutive population spikes.

The selection of events was performed using filtered data superimposed on unfiltered data to ensure that possible filtering artifacts would not contaminate the analysis. The population spike interval data from 15 animals was then pooled and subsequently grouped according to stimulation β burst frequency. We conducted a one-way analysis of variance (SPSS Inc.) against the stimulation frequencies to define stimulation frequency dependent differences in mean frequencies across frequency bands. Tukey-test was used for post hoc analyses.

CSD analysis was calculated according to Freeman and Nicholson (1975) in Matlab (MathWorks Inc.). The CSD was calculated as $CSD(z)=[(2f(z)-f(z+\Delta z)-f(z-\Delta z)]\sigma z/(\Delta z)^2$, where $CSD(z)$ is the CSD at depth z, $f(z)$ is the local field potential at depth z, Δz is the depth interval (Timofeev and Steriade, 1997) and σz is the conductivity along the shaft of the 16-channel recording electrode. Conductivity was not measured during the experiments, but was considered as constant across hippocampal subfields. The resulting error can be considered as negligible with respect to the kind of results we sought (Holsheimer, 1987; Wadman et al., 1992; Kaibara and Leung, 1993). Thus, CSDs were calculated in arbitrary units (mV/mm^2), proportional to the actual current densities (Kaibara and Leung, 1993). Averaged 50 ms CSDs were calculated from four 20 s epileptiform afterdischarges and traces of non-epileptiform evoked potentials of equal length.

Autocorrelation and coherence were calculated for 10-fold downsampled signals using Matlab signal processing toolbox (MathWorks Inc.). Autocorrelation was calculated on CA1 inter-spike interval data pooled from eight animals. Only events occurring later than 2 s after cessation of the stimulation were considered as discharges and included into the autocorrelation analysis. The statistical significance of the correlation was evaluated between frequency bands using one-way analysis of variance (SPSS Inc.). For coherence, signals corresponding to CA1 and DG were pre-selected on the basis of the CSD analysis. Coherence was calculated on 20 s mean epileptiform voltage trace pooled from three perforant path and fimbria fornix stimulations. The window for the analysis was 1 s and it was moved a sample at a time across the entire 20 s signal. Three 20 s voltage traces of spontaneous oscillations collected prior to the stimulation experiments were used as reference for normal coherence under urethane anesthesia. Standard error of mean described the inter-discharge variation.

For time-frequency analysis we used wavelets on CA1 voltage data downsampled to 1 kHz. Time-frequency analysis was calculated in Matlab (MathWorks Inc.) according to Muthuswamy and Thakor (1998). Morlet wavelets were calculated from 0.1 Hz to 60 Hz with 0.1 Hz resolution in frequency domain and 1 kHz resolution in temporal domain. We imaged both spontaneous oscillations an individual afterdischarge to demonstrate the differences in the intensity and frequency distribution between normal and epileptiform *in vivo* rhythms of urethane anesthetized rat hippocampus.

RESULTS

Stimulation paradigm of the experiment (Fig. 1) was designed to correspond to the frequency relationships between different epileptic oscillatory brain states (Pare et al., 1992; Steriade and Contreras, 1998; Bikson et al., 2003). β Burst stimulation delivered at 10 min intervals at twice the threshold capable of inducing population spikes was sufficient to drive the hippocampal neuronal network into epileptiform state during the first 2 h of the stimulations in all but one of the recorded animals. We defined the emergence of a depolarizing shift as the beginning of an epileptiform afterdischarge (Somjen et al., 1985). Thereby afterdischarges always initiated first at DG regardless of the stimulation site. In addition, the population excitatory postsynaptic potentials increased three-fold at the initiation of the afterdischarge (data not shown). On each recording day, both fimbria fornix and perforant path stimulations were continued until induced afterdischarges emerged. Inter-animal variance between trials was too large to reveal any differences in the afterdischarge thresholds between different stimulation sites. In general, three to six 64 pulse stimulation series with 10 min intervals were required before the afterdischarges emerged.

CSD analysis

CSDs were used to identify different hippocampal subfields. In addition, CSD analyses were used to evaluate the propagation of field potentials and discharges during and after the stimulations (Fig. 2) and averaged to accurately describe the locations of sources and sinks (Fig. 3). Thereafter, discharges were classified according to the CSD analyses.

The first DG population spikes induced by perforant path stimulation did not propagate from DG to CA1 (Figs. 2A and 3A). However, perforant path stimulation induced a minute population spike in CA1 5 ms after the stimulation. Fimbria fornix stimulation, on the other hand, induced immediate population spikes at CA1 (Fig. 3C), but did not induce DG firing until 1–3 s later (Fig. 2D). At the emergence of the epileptiform afterdischarge the propagation profile transformed as described in Somjen et al. (1985). The early discharges still had the overall temporal profile of the normal transmission of action potentials through the hippocampal trisynaptic loop. Five seconds from the onset of the afterdischarge the temporal sequence of events was already compromised as evidenced by the nearly vertical dashed lines indicating the individual population spikes in Fig. 2B and E.

As reported previously (see Jefferys, 2003, for review), the temporal differences between hippocampal subfields vanished during the progression of the self-sustained epileptiform afterdischarge and were completely replaced by region specific and nearly synchronous population spike sinks in the hippocampal subfields irrespective of the stimulation site (Figs. 2C, F, 3B, D). The CA1 basal dendritic sinks increased as the time difference between DG and CA1 spike discharges decreased (compare Fig. 2B, C, E, F). These large basal sinks can also be seen in averaged CSDs after fimbria fornix stimulation (Fig. 3C) and during epileptiform afterdischarges (Fig. 3B, D). Additionally, the origin of the synchronous population spike discharge sinks varied between DG and CA1 (Fig. 2B, C, E, F). Interestingly, the average profiles of perforant path and fimbria fornix stimulation induced afterdischarges were identical and resembled the CSD profile of the non-epileptiform evoked fimbria fornix stimulation (Fig. 3). Since the overall profiles and frequencies of the epileptiform afterdischarges obtained by stimulating perforant path and fimbria fornix were inherently similar, they have been pooled in the subsequent analyses.

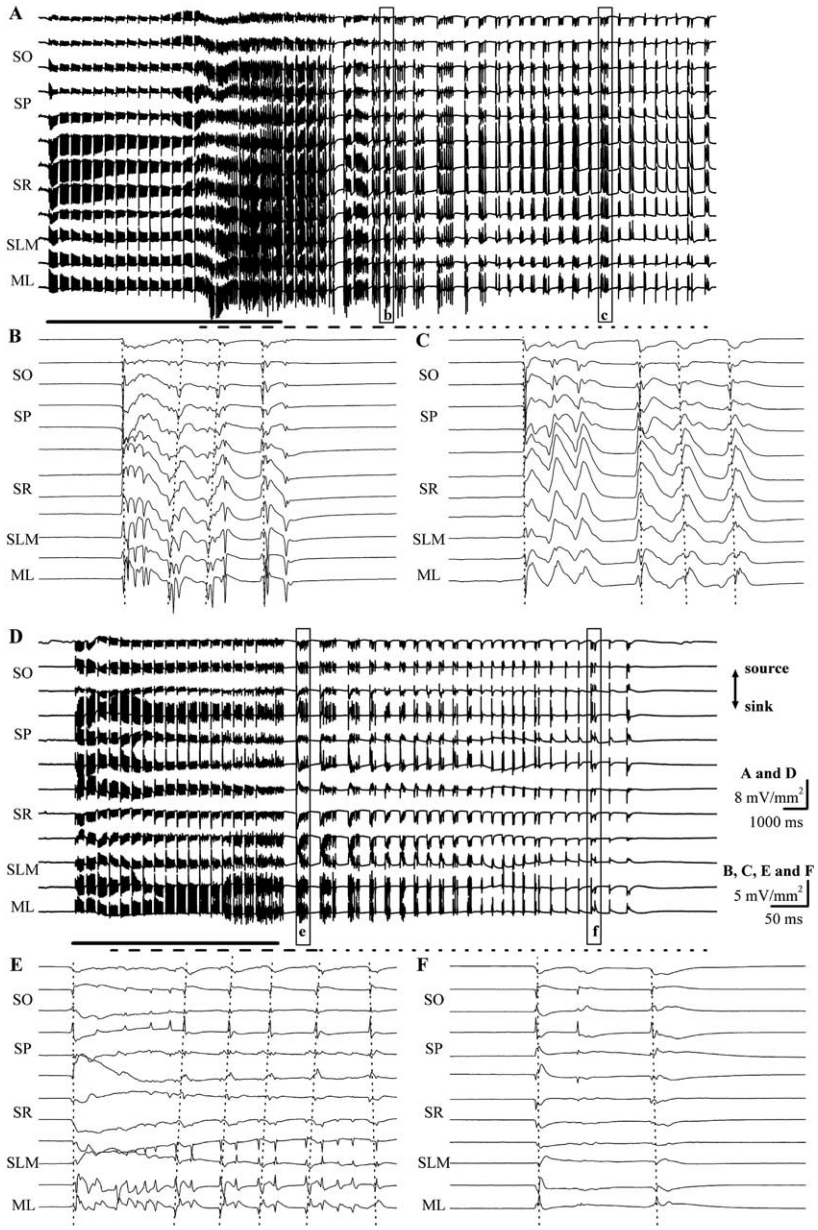

Fig. 2. CSD analysis of β burst stimulation induced afterdischarge switching from synaptic propagation into region specific, nearly synchronous discharges in hippocampus. (A and D) CSD clips of 12 channels from epileptiform afterdischarge induced by 20 Hz β burst stimulation of perforant path (A) and fimbria fornix (D). Here, and in subsequent figures, the time of the stimulation is indicated as a solid black line, the temporal span of discharges that propagate in temporally normal order is presented as a dashed line and the nearly simultaneous regionally independent discharges between the hippocampal subfields are indicated as a dotted line. Note the depolarizing wave at 6 s (A) and 2 s (D) initiating the afterdischarges. The symbols on the left of the trace in this and subsequent figures denote stratum oriens (SO), s. pyramidale (SP), s. radiatum (SR), s. lacunosum moleculare (SLM), and molecular layer of the DG (ML). Note the different initial response patterns governed by SLM and ML in perforant path stimulation (A) and SP and SR in fimbria fornix stimulation (D). Note also that although the discharge patterns and temporal relations of the different stimulations are similar, the SLM is source in perforant path stimulation (A) and sink in fimbria fornix stimulation (D). Note also the differential slow wave changes in the current-depth profiles between stimulation sites. Dashed boxes around the trace indicate the time points of the magnified insets (B), (C), (E) and (F). (B and E) The discharges initiate at DG, and the CA1 population spikes are mainly synaptically mediated indicated by dashed lines originating at DG and propagating into CA1. Note that the first population spike discharge of each burst is simultaneous at DG and CA1. The subsequent discharges in the burst have irregular time difference between DG and CA1. (C and F) The delayed discharge is composed of region specific and nearly synchronous discharges at CA1 and DG. In addition, an increase in size and duration of the apical dendritic sinks in SR is associated with the epileptiform discharges. Note the minute variation in the time-lags between the different hippocampal subfields and the changes in the direction of the discharge propagation, where CA1 population spikes can precede DG, or vice versa.

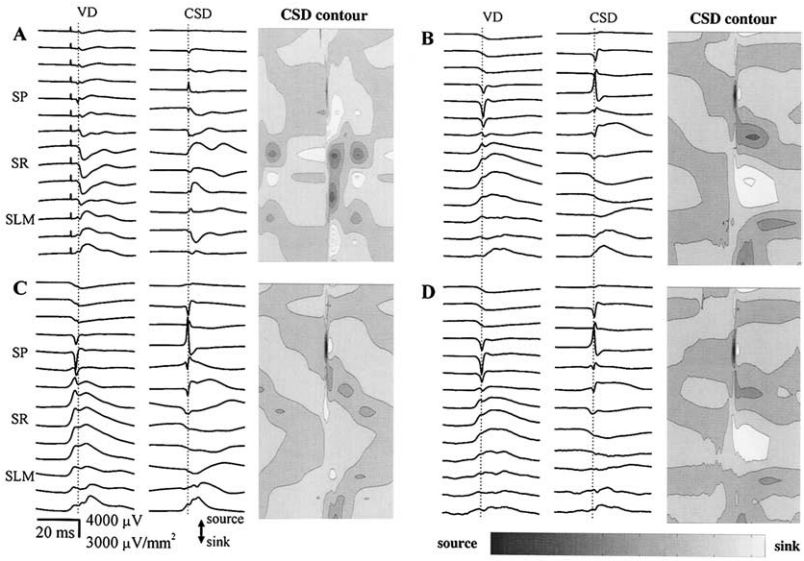

Fig. 3. CSD analysis of the averaged evoked and epileptiform spikes. Each trace is an average of 200 50 ms sweeps from two separate measurements. Notations on top of the figure denote voltage trace (VD) and CSD. Vertical dotted line in each panel indicates the position of the CA1 population spike peak used to trigger the averages. (A) Evoked response to perforant path stimulation. Perforant path stimulation induced a sink in SLM and sources in SR. Note the small population spike in CA1 5 ms after the stimulation, which may indicate a direct entorhinal connection. (B) Epileptiform response to perforant path stimulation. Epileptiform afterdischarge had a population spike in SP and the large sink in SR. (C) Evoked response to fimbria fornix stimulation. Fimbria fornix stimulation evoked a population spike related sink in SP and a small sink in proximal SR. Note also that the stimulation artifacts have nearly vanished due to the averaging. (D) Epileptiform response to fimbria fornix stimulation. Epileptiform afterdischarge had a population spike associated sink in SP and the large sink in SR. Note also the minute sink in SLM. Note also the remarkable similarity between (B) and (D) as well as their close resemblance to (C).

Stimulation frequencies

One-way analysis of variance was calculated for epileptiform spike discharge intervals from CA1 voltage recordings from 20 animals. Population spike intervals were defined as the time difference between two consecutive population spikes (N=3071) for the whole time series of all β burst stimulation frequencies after removal of stimulation artifacts. The variance analysis revealed no significant differences in population spike discharge frequencies between different stimulation frequencies. We wanted to further examine the frequency profile of the discharges by grouping them into five frequency groups: Δ, θ, β, γ, and fast. β Frequency discharges accounted for 46% of all the frequencies assigning β frequencies as the single largest group of the analysis at every stimulation frequency. For β frequency band, mean (±95% confidence intervals) afterdischarge frequencies were 20.9±2.3 Hz, 19.7±3.3 Hz, and 20.7±1.9 Hz, respectively for 14, 17, and 20 Hz stimulation frequencies. A change of the stimulation β frequency between 14, 17, and 20 Hz had no effect on the prevalence of the afterdischarges.

Discharge frequencies

Autocorrelation analyses were conducted for extracellular single channel recordings of β burst stimulation induced CA1 afterdischarges pooled from eight animals with the longest afterdischarges (Fig. 4). For autocorrelation analysis, only discharges occurring 2 s after the cessation of the stimulation were included into the analysis. Therefore, the autocorrelation data were not contaminated by any direct or indirect stimulatory artifacts. Autocorrelation demonstrated that β burst stimulation induced epileptiform afterdischarges peaking at 200, 20, and 2 Hz (Fig. 4A). The profile of the afterdischarge is presented in Fig. 4B, whereas the 2 Hz Δ frequencies can be seen in Fig. 4C. Fig. 4D demonstrates the 200 Hz frequencies and the early γ frequency bursting. The second spike in the 200 Hz fast frequencies was usually smaller than the first spike. The steady β frequency component within the afterdischarge is exemplified in Fig. 4E. Interestingly, although γ frequency firing was present in the beginning of the afterdischarge (Fig. 4D), the autocorrelation demonstrated a relative reduction of incidences at γ and θ frequencies.

Coherence during the epileptiform afterdischarge

In order to study the development of the ultrasynchronous events across the hippocampal subfields, 10-fold downsampled epileptiform voltage traces pre-selected on the basis of CSD analysis and corresponding to the principal cell layers of CA1 and DG were selected for coherence analysis (Fig. 5). Fig. 5A, pooled from three animals, demonstrates that in spontaneous oscillations in rat hippocampus under urethane anesthesia γ frequencies are prevalent and the coherence values are lower compared with the afterdischarges. Fig. 5B demonstrates the pooled coherence from three epileptiform afterdischarges. The coherence is strong at slow and β frequencies, but there is little coherence at γ or high frequencies. There is also a slight drop in the coherence at θ frequencies in Fig. 5B.

Temporal succession of alterations in the frequency content of the afterdischarge

We wanted to monitor the epileptiform afterdischarge simultaneously in frequency and time in order to capture the tem-

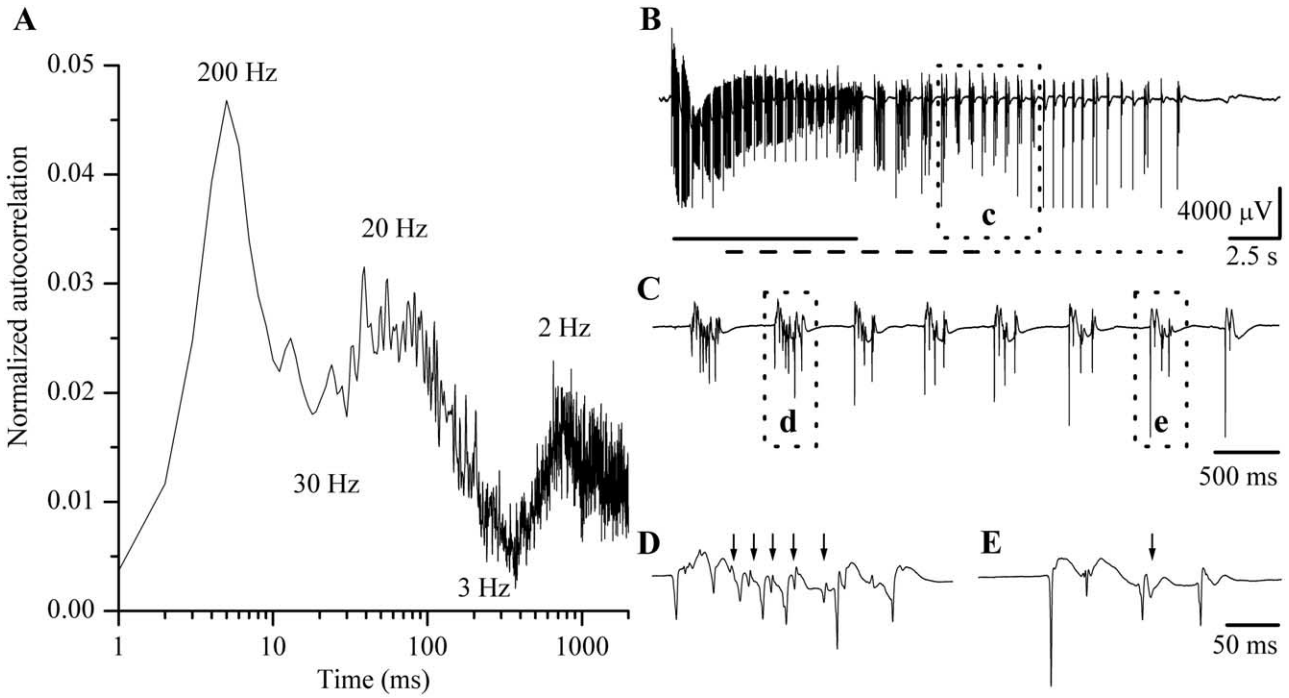

Fig. 4. Autocorrelation of CA1 population spike discharges after β burst stimulation pooled from eight animals. (A) Autocorrelation of the discharges. Note the logarithmic scale on *x* axis. First 2 s of the afterdischarges were omitted from the analysis in order to obtain discharges that did not contain stimulatory artifacts or desynchrony from transition into epileptiform state. Note the positive peaks at 200, 20, and 2 Hz positions and the negative peaks of the signal at γ and θ frequencies. The frequency bands with positive peaks are significantly different from frequency bands with negative peaks (one-way analysis of variance, $N=831$, $P<0.05$). (B) An example of the afterdischarge. See Fig. 2 for details of the lines beneath the figure. Dashed box around the trace indicates the time point of the magnified inset (C). (C) Inset from (B) indicating the 2 Hz slow frequency. Dashed boxes around the trace indicate the time points of the magnified insets (D) and (E). (D) Inset from (C) indicating the fast 200 Hz activity in the CA1 as vertical arrows. Note also the γ frequency spikes present in the beginning of the afterdischarge and their transitioning into β frequencies. (E) Inset from (C) demonstrating the β frequency discharges.

poral structure of the alterations in frequency domain. The time-frequency analysis was calculated using wavelets (Muthuswamy and Thakor, 1998). To visualize the differences between normal and epileptiform CA1 activity we imaged a spontaneous 20 s trace of local field potentials (Fig. 6A, B) and a single epileptiform afterdischarge (Fig. 6C, D). These results are applicable to all 20 animals recorded. The field potentials mainly consisted of θ frequencies (Fig. 6B). In the afterdischarge, there was an initial discharge at γ frequencies coinciding with the depolarizing shift (Fig. 6C, D, starting from line i). Next the γ discharge was accompanied by an increasing β frequency component and a Δ frequency pattern emerged (Fig. 6C, D, line d). Thereafter the discharge transitioned into a prolonged and steady β frequency discharge (Fig. 6C, D, line b). Finally the afterdischarge terminated at a weaker burst of γ frequencies.

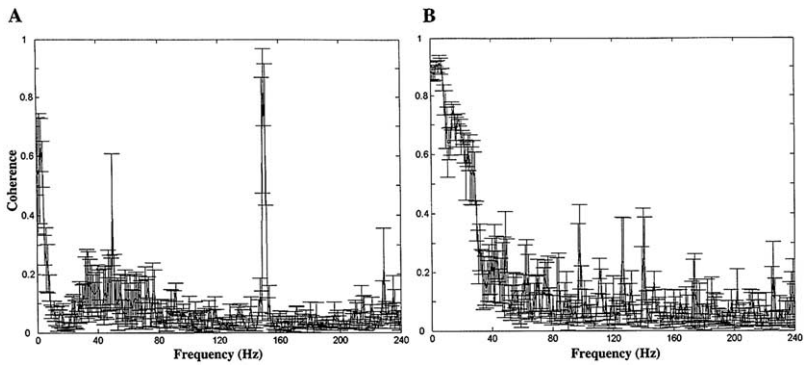

Fig. 5. Coherence analysis of normal and epileptiform rat hippocampus. (A) Coherence (±S.E.) of three 20 s traces of spontaneous field potentials from CA1 and DG. During spontaneous oscillations under urethane anesthesia coherence values peak at slow and γ frequencies. Note also the 50 and 150 Hz interference from fluorescent lamps. (B) Coherence (±S.E.) of three afterdischarges recorded from CA1 and DG. During the afterdischarges the coherence at Δ and β frequencies is high, but declines rapidly at γ frequencies. Note also the slight reduction of coherence at θ frequency.

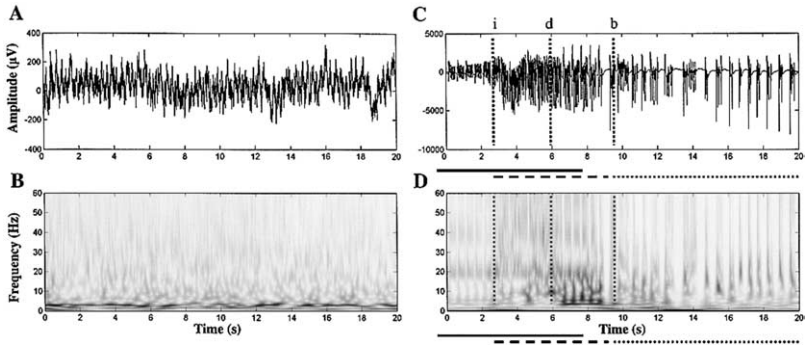

Fig. 6. Time-frequency evolution of the CA1 voltage traces by wavelet transformation. (A) A voltage trace of spontaneous oscillations recorded from CA1. (B) A wavelet transformation of (A). Note the strong θ frequency oscillation. (C) A voltage trace of CA1 epileptiform discharges. (D) A wavelet transformation of (C). The vertical dotted lines in (C) and (D) indicate the timing of the frequency switches associated with initiation of the discharge (i), emergence of Δ rhythm (d), and the steady β frequency discharge (b). See Fig. 2 for details of the lines beneath (C) and (D). The discharges are characterized by strong Δ and β frequency drives. In addition, initial and terminal phases of the discharges are accompanied by γ frequencies that are higher harmonics of the underlining β frequency drive.

DISCUSSION

Analysis of discharges of ensembles of neurons firing in unison provides a time-sensitive means to investigate the emergence of synchronized neuronal activity. We aimed to benefit from the temporal accuracy of these discharges within hippocampal subfields to examine the emergence of epileptiform afterdischarges at different frequency bands. Our results show that β burst stimulation efficiently induces epileptiform afterdischarges in urethane anesthetized rat hippocampus *in vivo*. These afterdischarges consist of early and late phases of γ frequency discharges that border a prolonged discharge at 200 Hz fast, 20 Hz β and 2 Hz Δ frequencies. These states seem to be mutually exclusive.

Roles of stimulation pattern, frequency, and site in the induction of afterdischarges

Although we artificially induced epileptiform afterdischarges using stimulation bursts at β and Δ frequencies, the initial innate neuronal network response of the hippocampus was a discharge at γ frequencies. Therefore, the necessary conditions for the epileptiform afterdischarge were generated by the β burst stimulation, but the innate neuronal network generated γ frequency discharges were required for the emergence of the actual epileptiform afterdischarge at fast, β, and Δ frequencies.

Our patterned β burst stimulation resembles previous fast kindling protocols (e.g. Bragin et al., 1997a), but benefits from the natural brain oscillations in the temporal structure of the stimulation and, furthermore, restricts the number of stimulation pulses into 384 in an hour and 2304 in a typical 6 h recording day. In this study we focused on maintaining the overall intensity of the stimulation as constant as possible and varied the stimulatory β frequency only at the central frequencies of the β frequency band. At our selection of frequencies the alteration of the stimulation frequency in the β burst had no observable effect on the prevalence or frequency of the consecutive afterdischarges. Our β burst model was able to induce epileptiform afterdischarges lasting over 10 s with three series of 64 stimulation pulses in naive rats under urethane anesthesia even though urethane is known to suppress glutamatergic transmission and promote anticonvulsive effects (Heltovics et al., 1995). Lothman and Williamson (1992) demonstrated that similar numbers of stimulations delivered without patterning could induce afterdischarges in already kindled rat. The fact that the 64 pulse stimulation series was to be repeated three times with 10 min intervals before afterdischarges emerged suggests that some slow changes take place within the brain to allow excessive excitation and epileptiform discharges. In other words, the overall duration of the stimulation must reach a critical threshold before afterdischarge can develop (Lothman and Williamson, 1992). Nevertheless, our β burst model shows that the efficacy of the stimulation can be improved by proper patterning of the stimulation pulses.

Both perforant path and fimbria fornix stimulations induced similar afterdischarges in the hippocampal neuronal network. Stimulation of either site induced an afterdischarge that had a large sink in distal stratum radiatum (SR) as evidenced by the CSD analysis. Similarly, the voltage traces demonstrated that CA1 was more profoundly activated than DG. The overall CSD profile of the afterdischarges resembled the profile from evoked non-epileptic fimbria fornix stimulation. However, the sinks in SR were stronger and longer and more distal during the epileptiform afterdischarges. The increased duration of the SR sink indicate reduced $GABA_A$ mediated inhibition in CA3-CA1 synapses at SR (Wu and Leung, 2003).

Hippocampal state switch

The transition from the normal state to epileptiform afterdischarges was accompanied with strong depolarizing waves and increased population excitatory postsynaptic potentials initiating the afterdischarge. The emergence of this depolarizing wave was stimulation site independent. Our observations are in accordance with Somjen et al. (1985), Buzsaki et al. (1989), Wadman et al., 1992, and Bracci et al. (2001). In addition, there was an early γ discharge similar to the γ activation of local circuits of the hippocampus previously described by Finnerty and Con-

nors (2000). An excessive glutamatergic activation of the hippocampal neuronal network has been shown to result in ultrasynchronous γ oscillation leading to epileptiform afterdischarges (Medvedev, 2001). In conjunction, synchronous activation of inhibitory synapses at γ frequency has been shown to accumulate chloride into pyramidal cells, thus reducing the efficacy of inhibitory potentials (Bracci et al., 2001). Similar reduction of inhibitory potentials was observable in the increased SR sinks in our CSD data during the epileptiform afterdischarge. Such conditions may aid the afterdischarge generation by challenging the inhibitory neuronal network.

Following the depolarizing wave we recorded a prevalent 10–20 s stable 21 (±2) Hz β frequency phase in the afterdischarge. Occasionally the network skipped a cycle resulting in 10 Hz β discharges present in the time-frequency and autocorrelation analyses. The possible mechanisms underlying epileptiform β frequencies are elusive (Miller, 1989; Pare et al., 1992; Charpak et al., 1995; Bracci et al., 1999; Traub et al., 1999; Jefferys, 2003).

The early γ frequency burst coincided with synaptic propagation of the population spikes, whereas the steady-state β afterdischarges were composed of individual but nearly synchronous population spikes. Furthermore, the autocorrelation analysis omitting the first 2 s of the afterdischarge revealed reduced levels of γ and θ frequencies. This suggests that the observed epileptiform γ and β oscillations represent two distinct oscillatory states that cannot coexist (Penttonen and Buzsaki, 2003). Correspondingly, Fellous and Sejnowski (2000) demonstrated that carbachol induced θ and Δ oscillations were mutually exclusive. It may be that the observed episodes of γ frequency activity represent transition phases bordering the actual epileptiform afterdischarge at β frequencies.

In our experiment, the synaptic propagation from DG to CA1 via CA3 was replaced by nearly simultaneous discharges at DG and CA1. These nearly synchronous discharges were initiated either in DG or CA1. Such non-sequential oscillation suggests the emergence of coupled oscillators (Finnerty and Jefferys, 2002; Jefferys, 2003). Formation of local oscillators is further supported by the fact that the β burst stimulation increased and spread the CA1 dendritic excitation in favor of more distal portions of the apical dendritic tree (Wu and Leung, 2003). The afterdischarge was terminated at γ frequencies as described in Bragin et al. (1997b), Penttonen et al. (1999), and Ma and Leung (2002).

The 200 Hz, 20 Hz, and 2 Hz oscillators

The CSD analysis revealed that the β burst stimulation induced a large sink in basal CA1 dendrites. Additionally, the 200 Hz high frequency activity present in the CA1 autocorrelation analysis was missing from the coherence analysis between CA1 and DG indicating that the high frequency activity was restricted to CA1 area. Both basal CA1 dendritic activation and the appearance of fast 200 Hz discharges coincided with the initiation of the epileptiform afterdischarge. This indicates that the recurrent CA1 basal dendritic activation could participate in the local 200 Hz rhythm in CA1 subfield by recurrent excitation or dendritic backpropagation. The varying amplitudes of the high frequency discharges, on the other hand, suggest that multiple small aggregates fire at an attempt to synchronize themselves prior to the β frequency transformation (Bikson et al., 2003). Increased β frequency activity may be the result of increased afterhyperpolarization associated with accumulation of extracellular potassium (Traub et al., 1999). Such accumulation could aid the formation of coupled oscillators in hippocampal subfields (Jefferys, 2003). Pare et al. (1992) and Barbarosie and Avoli (1997) have reported synchronous Δ frequency discharges in entorhinal cortex and hippocampus. This suggests that the Δ rhythm may involve larger partially extrahippocampal coupled oscillators. This could explain the differential Δ wave patterns during perforant path and fimbria fornix stimulations present in Fig. 2. Furthermore, the response frequencies reported in this paper for hippocampal afterdischarges (200, 20, 2 Hz) have been shown to optimally induce long term potentiation in deep layers of the entorhinal cortex (Yun et al., 2002).

CONCLUSIONS

We demonstrate in this article that *in vivo* β burst stimulation induces epileptiform afterdischarges peaking at 200, 20, and 2 Hz with a prominent β frequency component. These afterdischarges are initiated and terminated at γ frequencies. We propose that these frequencies correspond to coupling of the epileptiform discharge at different spatial extents or neuronal distances. Hippocampal subfield specific discharges exploit 150–250 Hz high frequencies, intrahippocampal coupled oscillators are formed at 10–30 Hz β frequencies and 1–2 Hz Δ frequencies recruit neuronal components outside the hippocampus. Similar dependency between frequency and cortical distance has been described previously in a model of oscillatory cortical circuits by Pinto et al. (2003). Such coupled oscillators that are inversely nested in size and frequency could explain the synchronicity at multiple levels of neuronal networks observed during epilepsy.

Acknowledgments—This work was supported by grants from Finnish Cultural Foundation and Kuopio University Fund (J.E.M.).

REFERENCES

Amzica F, Steriade M (1999) Spontaneous and artificial activation of neocortical seizures. J Neurophysiol 82:3123–3138.

Barbarosie M, Avoli M (1997) CA3-driven hippocampal-entorhinal loop controls rather than sustains in vitro limbic seizures. J Neurosci 17:9308–9314.

Bikson M, Fox JE, Jefferys JG (2003) Neuronal aggregate formation underlies spatiotemporal dynamics of nonsynaptic seizure initiation. J Neurophysiol 89:2330–2333.

Bracci E, Vreugdenhil M, Hack SP, Jefferys JG (1999) On the synchronizing mechanisms of tetanically induced hippocampal oscillations. J Neurosci 19:8104–8113.

Bracci E, Vreugdenhil M, Hack SP, Jefferys JG (2001) Dynamic modulation of excitation and inhibition during stimulation at gamma and beta frequencies in the CA1 hippocampal region. J Neurophysiol 85:2412–2422.

Bragin A, Csicsvari J, Penttonen M, Buzsaki G (1997a) Epileptic afterdischarge in the hippocampal-entorhinal system: current source density and unit studies. Neuroscience 76:1187–1203.

Bragin A, Penttonen M, Buzsaki G (1997b) Termination of epileptic afterdischarge in the hippocampus. J Neurosci 17:2567–2579.

Buzsaki G (1989) Two-stage model of memory trace formation: a role for "noisy" brain states. Neuroscience 31:551–570.

Buzsaki G, Ponomareff GL, Bayardo F, Ruiz R, Gage FH (1989) Neuronal activity in the subcortically denervated hippocampus: a chronic model for epilepsy. Neuroscience 28:527–538.

Charpak S, Pare D, Llinas R (1995) The entorhinal cortex entrains fast CA1 hippocampal oscillations in the anaesthetized guinea-pig: role of the monosynaptic component of the perforant path. Eur J Neurosci 7:1548–1557.

Fellous JM, Sejnowski TJ (2000) Cholinergic induction of oscillations in the hippocampal slice in the slow (0.5–2 Hz), theta (5–12 Hz), and gamma (35–70 Hz) bands. Hippocampus 10:187–197.

Finnerty GT, Connors BW (2000) Sensory deprivation without competition yields modest alterations of short-term synaptic dynamics. Proc Natl Acad Sci USA 97:12864–12868.

Finnerty GT, Jefferys JG (2002) Investigation of the neuronal aggregate generating seizures in the rat tetanus toxin model of epilepsy. J Neurophysiol 88:2919–2927.

Freeman JA, Nicholson C (1975) Experimental optimization of current source-density technique for anuran cerebellum. J Neurophysiol 38:369–382.

Heltovics G, Boda B, Szente M (1995) Anticonvulsive effect of urethane on aminopyridine-induced epileptiform activity. Neuroreport 6:577–580.

Hirai N, Uchida S, Maehara T, Okubo Y, Shimizu H (1999) Beta-1 (10–20 Hz) cortical oscillations observed in the human medial temporal lobe. Neuroreport 10:3055–3059.

Holsheimer J (1987) Electrical conductivity of the hippocampal CA1 layers and application to current-source-density analysis. Exp Brain Res 67:402–410.

Jefferys JG (2003) Models and mechanisms of experimental epilepsies. Epilepsia 44 (Suppl 12) 44–50.

Kaibara T, Leung LS (1993) Basal versus apical dendritic long-term potentiation of commissural afferents to hippocampal CA1: a current-source density study. J Neurosci 13:2391–2404.

Liang H, Bressler SL, Ding M, Truccolo WA, Nakamura R (2002) Synchronized activity in prefrontal cortex during anticipation of visuomotor processing. Neuroreport 13:2011–2015.

Lothman EW, Williamson JM (1992) Influence of electrical stimulus parameters on afterdischarge thresholds in the rat hippocampus. Epilepsy Res 13:205–213.

Ma J, Leung LS (2002) Metabotropic glutamate receptors in the hippocampus and nucleus accumbens are involved in generating seizure-induced hippocampal gamma waves and behavioral hyperactivity. Behav Brain Res 133:45–56.

Markram H, Lubke J, Frotscher M, Sakmann B (1997) Regulation of synaptic efficacy by coincidence of postsynaptic APs and EPSPs. Science 275:213–215.

McCormick DA, Contreras D (2001) On the cellular and network bases of epileptic seizures. Annu Rev Physiol 63:815–846.

Medvedev A, Mackenzie L, Hiscock JJ, Willoughby JO (2000) Kainic acid induces distinct types of epileptiform discharge with differential involvement of hippocampus and neocortex. Brain Res Bull 52:89–98.

Medvedev AV (2001) Temporal binding at gamma frequencies in the brain: paving the way to epilepsy? Australas Phys Eng Sci Med 24:37–48.

Mikkonen JE, Gronfors T, Chrobak JJ, Penttonen M (2002) Hippocampus retains the periodicity of gamma stimulation in vivo. J Neurophysiol 88:2349–2354.

Miller R (1989) Cortico-hippocampal interplay: self-organizing phase-locked loops for indexing memory. Psychobiology 17:115–128.

Muthuswamy J, Thakor NV (1998) Spectral analysis methods for neurological signals. J Neurosci Methods 83:1–14.

Pare D, deCurtis M, Llinas R (1992) Role of the hippocampalentorhinal loop in temporal lobe epilepsy: extra- and intracellular study in the isolated guinea pig brain in vitro. J Neurosci 12:1867–1881.

Penttonen M, Buzsaki G (2003) Natural logarithmic relationship between brain oscillators. Thal Relat Syst 2:145–152.

Penttonen M, Nurminen N, Miettinen R, Sirvio J, Henze DA, Csicsvari J, Buzsaki G (1999) Ultra-slow oscillation (0.025 Hz) triggers hippocampal afterdischarges in Wistar rats. Neuroscience 94:735–743.

Pinto DJ, Jones SR, Kaper TJ, Kopell N (2003) Analysis of state-dependent transitions in frequency and long-distance coordination in a model oscillatory cortical circuit. J Comput Neurosci 15:283–298.

Sirota A, Csicsvari J, Buhl D, Buzsaki G (2003) Communication between neocortex and hippocampus during sleep in rodents. Proc Natl Acad Sci USA 100:2065–2069.

Somjen GG, Aitken PG, Giacchino JL, McNamara JO (1985) Sustained potential shifts and paroxysmal discharges in hippocampal formation. J Neurophysiol 53:1079–1097.

Steriade M, Contreras D (1998) Spike-wave complexes and fast components of cortically generated seizures: I. Role of neocortex and thalamus. J Neurophysiol 80:1439–1455.

Steriade M, McCormick DA, Sejnowski TJ (1993) Thalamocortical oscillations in the sleeping and aroused brain. Science 262:679–685.

Timofeev I, Grenier F, Steriade M (1998) Spike-wave complexes and fast components of cortically generated seizures: IV. Paroxysmal fast runs in cortical and thalamic neurons. J Neurophysiol 80:1495–1513.

Timofeev I, Steriade M (1997) Fast (mainly 30–100 Hz) oscillations in the cat cerebellothalamic pathway and their synchronization with cortical potentials. J Physiol 504:153–168.

Traub RD, Whittington MA, Buhl EH, Jefferys JG, Faulkner HJ (1999) On the mechanism of the gamma→beta frequency shift in neuronal oscillations induced in rat hippocampal slices by tetanic stimulation. J Neurosci 19:1088–1105.

Wadman WJ, Juta AJ, Kamphuis W, Somjen GG (1992) Current source density of sustained potential shifts associated with electrographic seizures and with spreading depression in rat hippocampus. Brain Res 570:85–91.

Wu K, Leung LS (2003) Increased dendritic excitability in hippocampal ca1 in vivo in the kainic acid model of temporal lobe epilepsy: a study using current source density analysis. Neuroscience 116:599–616.

Yun SH, Mook-Jung I, Jung MW (2002) Variation in effective stimulus patterns for induction of long-term potentiation across different layers of rat entorhinal cortex. J Neurosci 22:1–5.

(Accepted 26 August 2004)